

Interaction of Tea Tree Oil with Model and Cellular Membranes

Cristiano Giordani, Agnese Molinari, Laura Toccaceli, Annarica Calcabrini, Annarita Stringaro, Pietro Chistolini, Giuseppe Arancia, and Marco Diociaiuti*

Dipartimento di Tecnologie e Salute, Istituto Superiore di Sanita', Viale Regina Elena 299, 00161 Roma, Italy

Received February 28, 2006

Tea tree oil (TTO) is the essential oil steam-distilled from *Melaleuca alternifolia*, a species of northern New South Wales, Australia. It exhibits a broad-spectrum antimicrobial activity and an antifungal activity. Only recently has TTO been shown to inhibit the in vitro growth of multidrug resistant (MDR) human melanoma cells. It has been suggested that the effect of TTO on tumor cells could be mediated by its interaction with the plasma membrane, most likely by inducing a reorganization of lipid architecture. In this paper we report biophysical and structural results obtained using simplified planar model membranes (Langmuir films) mimicking lipid “rafts”. We also used flow cytometry analysis (FCA) and freeze-fracturing transmission electron microscopy to investigate the effects of TTO on actual MDR melanoma cell membranes. Thermodynamic (compression isotherms and adsorption kinetics) and structural (Brewster angle microscopy) investigation of the lipid monolayers clearly indicates that TTO interacts preferentially with the less ordered DPPC “sea” and that it does not alter the more ordered lipid “rafts”. Structural observations, performed by freeze fracturing, confirm that TTO interacts with the MDR melanoma cell plasma membrane. Moreover, experiments performed by FCA demonstrate that TTO does not interfere with the function of the MDR drug transporter P-gp. We therefore propose that the effect exerted on MDR melanoma cells is mediated by the interaction with the fluid DPPC phase, rather than with the more organized “rafts” and that this interaction preferentially influences the ATP-independent antiapoptotic activity of P-gp likely localized outside “rafts”.

Introduction

Tea tree oil (TTO) is the essential oil steam-distilled from *Melaleuca alternifolia*, a species native to northern New South Wales, Australia. TTO consists of a complex mixture of monoterpenoids of which about 50% are oxygenated and about 50% are hydrocarbons.¹ The oil is considered nontoxic, it has a pleasant odor and it is included in a wide range of products for skin and wound care. In fact, the oil's lipophilic nature enables it to penetrate the skin, suggesting it may be suitable for topical therapeutic use in the treatment of fungal mucosal and cutaneous infections. TTO exhibits broad-spectrum antimicrobial activity² that can be principally attributed to terpinen-4-ol^{3,4} and there are susceptibility data on a wide range of Gram-positive and -negative bacteria.^{5–10} Moreover, the antifungal activity of TTO against yeasts and dermatophytes is reported in several papers.^{11–14} Despite great interest in this substance, TTO has not been systematically studied in terms of structural chemistry, and its mechanism of action is still under investigation.

Calcabrini et al.¹⁵ recently described a promising antitumoral activity exerted by TTO. In particular, it was demonstrated that TTO inhibits the in vitro growth of human melanoma cells, by inducing caspase-dependent programmed cell death. A noteworthy finding was that the oil appeared to be more effective on drug-resistant melanoma cells, which expressed high levels of the drug transporter P-glycoprotein (P-gp) on the plasma membrane. P-gp plays an important role in drug distribution and elimination and, when overexpressed, may confer multidrug resistance (MDR). Studies have also provided evidence for a more general antiapoptotic function for P-gp, overcoming resistance to caspase-dependent apoptosis exerted by the drug transporter, even if the molecular events underpinning this

proposed function have not yet been carefully assessed.^{16–18} Preliminary ultrastructural observations suggest that the effect of TTO on tumor cells could be mediated by its interaction with the plasma membrane, likely through inducing a reorganization of lipid architecture.¹⁵

The role of membrane lipids in cellular function has recently been deeply revised. The classic fluid mosaic model¹⁹ has been enriched by greater focus on the role played by the different kinds of lipids. In 1985 Thompson and Tillack²⁰ proved that glycosphingolipids (GSL) may form domains. This has become the starting point for the investigation of naturally occurring lipid aggregation in the cellular membrane. In 1997 Simons and Ikonen²¹ proposed a model for the formation of the so-called “rafts”, dynamic assemblies of sphingolipids and cholesterol surrounded by a “sea” of glycerolipids. The “raft” hypothesis has since been a hot issue in modern biophysics.^{22–28} Lipid “rafts” were supposed to be mainly localized in the exoplasmic face (EF) of the cellular membrane, and the main role proposed was the activation of membrane proteins, such as P-gp, involved in many important membrane activities.

It has been recently demonstrated that the acquisition of MDR is accompanied by up regulation of lipids and proteins that constitute lipid “rafts” and “caveolar” membranes, notably glucosylceramide and caveolin.²⁹ These changes may be related to the finding that, in MDR cells, a significant fraction of cellular P-gp (about 40%) is associated with “rafts” domains and that both P-gp localization and ATP-ase activity seem to be modulated by cholesterol alterations.^{30,31} Thus, “rafts” association of P-gp appears to be of functional significance because its modulation markedly affected drug pumping.³⁰ It is worth noting that from these studies it appears evident that more than 50% of P-gp is not “raft” associated and could play a different functional role. In fact, very recently Radeva et al.³² found that P-gp is localized in particular lipid domains distinct from the

* Corresponding author. Fax: +39 06 49387140; Tel: +39 06 49902981; E-mail: marco.diociaiuti@iss.it; web site: www.iss.it.

classical “rafts” showing that P-gp and monosialoganglioside- G_{M1} (G_{M1}), a typical component of the classic “rafts”, did not colocalize.

Given these factors, better knowledge of the interaction between TTO and lipid “rafts” should contribute to clarify the mechanism of action of the oil.

We performed a biophysical and structural study using simplified planar model membranes (Langmuir films) to investigate the effects of TTO on lipid membranes. Planar model membranes, prepared by the Langmuir method, have been widely used to study the aggregation physics of lipids constituting an actual cellular membrane and their interaction with several proteins.^{33,34} The Langmuir trough, used to prepare the planar model at the air–water interface, allows the investigation of phase behavior and molecular organization of the lipids by measuring compression isotherms. Moreover, adsorption kinetics of substances injected in the water subphase can be obtained by monitoring the changes occurring in the pressure film over time.³⁵

Our aim was to investigate the effects induced by TTO on model membranes made of a mixture of dipalmitoylphosphatidylcholine (DPPC), G_{M1} , and cholesterol. As previously reported by Yuan and Johnston,²⁵ G_{M1} and cholesterol form ordered lipid domains in DPPC planar monolayers mimicking lipid “rafts”. To verify preferential interaction of TTO with “rafts”, experiments on plain DPPC Langmuir films were also performed, under the same experimental conditions used for the more complex mixture. Moreover, the two-dimensional Langmuir film morphology at the water–air interface was visualized, in real time, before and after the interaction with the oil, using Brewster angle microscopy (BAM).^{36,37}

Our biophysical results indicate that TTO interacts preferentially with the less ordered DPPC “sea” and that it does not dramatically alter the more ordered structure of “rafts”.

On the basis of this consideration, and bearing in mind that the P-gp functionality responsible for drug transport (MDR) is structurally correlated with “rafts”, we hypothesize that the previously observed antiapoptotic effect exerted by TTO on MDR resistant cells¹⁵ was mainly due to the activity of the existing fraction of P-gp not localized in the “rafts”; this fraction is most likely localized in the particular membrane microdomains distinct from the classical “rafts”, as recently proposed in the literature.³² To verify this hypothesis, we used freeze-fracturing (FF) transmission electron microscopy (TEM) to study the ultrastructural architecture of resistant human melanoma cell (M14 ADR) cell membranes to evaluate the effects induced by increasing concentrations of TTO. Finally, we applied flow cytometry analysis (FCA) to investigate the effects exerted by TTO on the drug transport activity of P-gp.

Results and Discussion

Langmuir Films and Brewster Angle Microscopy. Compression isotherms of the Langmuir films prepared with plain DPPC, G_{M1} , cholesterol, and the mixture mimicking the lipid “rafts”,²⁵ are reported in Figure 1. The curve for plain DPPC is characterized by a typical plateau located at about $p = 7$ mNm, due to the coexistence of the liquid expanded (LE) and liquid condensed (LC) phases, and by a collapse value of about 73 mNm, where the film is irreversibly damaged.³⁸ The isotherm for G_{M1} appears quite different, without the typical DPPC plateau and characterized by a collapse pressure of less than 70 mNm. The G_{M1} curve is shifted toward higher mean molecular area (MMA) values, due to the larger size of the G_{M1} molecule compared to the DPPC. The cholesterol curve appears very

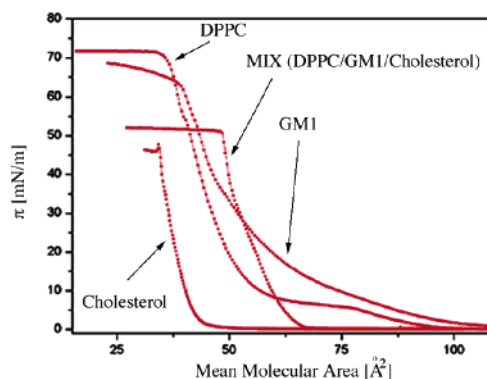


Figure 1. Compression isotherms. Typical isotherms of the plain components DPPC, cholesterol, and G_{M1} together with the isotherm obtained for the mixture (DPPC/ G_{M1} /cholesterol) mimicking the occurrence of lipid “rafts”.

different, with a very sharp collapse pressure of about 46 mNm, with no plateau and located at low MMA values due to small molecule size. The curve for the DPPC/ G_{M1} /cholesterol mixture (49/4/47 mol %) is in good agreement with the isotherm reported in the literature.²⁵ In particular, the curve lacks the typical plateau of DPPC, and its shape looks like the cholesterol isotherm and, more interestingly, is characterized by a collapse pressure of about 53 mNm, which lies between the cholesterol and the G_{M1} /DPPC collapse pressures. This behavior has been described in the literature and indicates that the collapsing film is an actual mixture of the three molecules.^{39,40} This observation confirms that we can prepare a Langmuir film mimicking the classical lipid “rafts”.

We now intend to study the interaction of this model membrane with TTO. Two different methods were used: (i) to mix TTO directly with lipids and deposit a Langmuir film; (ii) to insert TTO (previously dissolved in ethanol at a concentration of 33.3% v/v) in the water subphase under a preformed lipid Langmuir film.

Isotherms obtained for films prepared following procedure (i) with TTO/DPPC molar ratios of $X = 0.2, 0.6,$ and $0.8,$ are reported in Figure 2B. As can be seen, all curves share the typical DPPC shape and the only difference is in the MMA axis values. More in particular, the same isotherm can always be obtained by taking into account the dilution introduced in the final solution by the presence of the TTO/ethanol molecules (by calculating the MMA values using the final TTO concentration). This observation suggests that the TTO molecules are not steadily bound to the DPPC and that they evaporate during film deposition, leaving only DPPC molecules at the water–air interface.

In fact, TTO is very volatile and very difficult to keep at the air–water interface. It is important to verify if a plain TTO Langmuir film can be deposited at the air–water interface and if the film is stable over time. Following the procedure used for the lipid films, we deposited a Langmuir film using the TTO/ethanol solution. Our results indicate that a plain TTO film can be formed but that it is very instable. We observe that the compression isotherm is characterized by a pressure rising located at very low MMA values (data not shown). We interpreted this fact as due to the solubility of the TTO/ethanol in water, allowing the drops released by the syringe to be dispersed in the subphase, losing many TTO molecules and forming a Langmuir film composed of only the few remaining TTO molecules. Figure 2A shows the evolution of the plain TTO film pressure in the time course, at fixed barriers. As expected, TTO evaporation is very high and, after about 50 min,

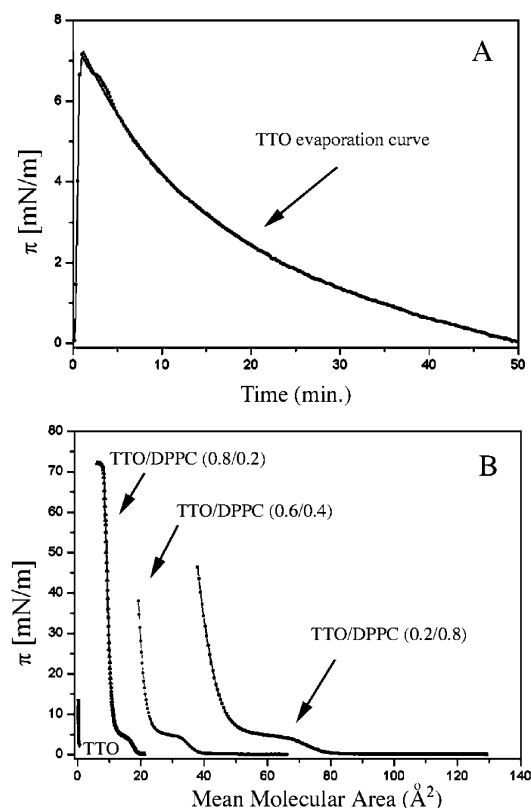


Figure 2. Forming Langmuir films with plain TTO (A) and mixtures DPPC/TTO (B). Time course behavior of the surface pressure of the plain TTO Langmuir film formed at the interface air–water (A) showing that the oil evaporates. Isotherms of mixtures DPPC/TTO with growing percentages of TTO are reported in (B). The isotherm shape is always the same and equal to the typical DPPC isotherm if divided by a scale factor, demonstrating that the oil evaporates during the film formation.

the pressure drops to zero suggesting that practically all TTO molecules evaporated. Results demonstrate that TTO molecules are dramatically volatile when air is accessible.

Procedure (ii) requires the injection of TTO molecules in the water subphase, previously dissolved in ethanol at a final concentration of 0.01, 0.02, 0.04% v/v (mother solution of 33.3% v/v for TTO in ethanol). The presence of TTO in the subphase dramatically changes the pressure of the lipid films preformed at the air–water interface. In particular, Figure 3A shows the effects induced on the DPPC film by the three different TTO concentrations, together with the relative BAM images. The injection of TTO in the subphase was performed at very low film pressure (barriers completely opened and DPPC in gaseous phase, as can be observed in the dark BAM image) and immediately raised the film pressure. Specifically, pressure reaches values ranging from 25 to 32 mNm, depending on the TTO concentration in the subphase. The TTO effect on film morphology is evident, as revealed by the three BAM images. The image background becomes gray and small white areas, typical of the lipid LC phase and similar to those observed in the plain DPPC at similar film pressure, become detectable.

The subsequent compression of the DPPC film, in the presence of TTO in the subphase, leads to isotherms reported in Figure 3A. The isotherm shape strongly depends on the TTO concentration.

At $X = 0.01$ and 0.02 a similar shape is observed, and the TTO concentration influences only the low MMA region. The collapse pressure is that of the plain DPPC and the presence of TTO molecules shifts only the collapse onset, from 47 to less

than 45 \AA^2 . A more evident effect is observed at $X = 0.04$. The insertion of TTO in the subphase induces a sharp rise in the film pressure (about 33 mNm) and changes the isotherm shape, still characterized by the DPPC collapse pressure value (about 72 mNm) but reached at a lower MMA value (about 40 \AA^2). BAM images revealed a high abundance of white areas that can be attributed to the lipid LC phase.

All observations indicate that TTO molecules interact with the preformed DPPC film in a dose-dependent manner. TTO molecules, coming from the water subphase, do not evaporate and penetrate the DPPC film. It is worth noting that, at all concentrations, the collapse pressure reaches the value typical of the plain DPPC (about 72 mNm), demonstrating that all films are made of DPPC molecules. The MMA value at which the collapse pressure is reached depends on the TTO concentration. Specifically, this value shifts toward low values when the TTO concentration rises. This is particularly evident at $X = 0.04\%$, even if a dose-dependent behavior exists at 0.01 and 0.02%. This indicates that the film rupture occurs at higher compressions when TTO molecules are more abundant.

The experiments described above for DPPC films were repeated with DPPC/ G_{M1} /cholesterol films, simulating classical lipid “rafts”. Results are summarized in Figure 3B.

First, BAM images for the Langmuir film without TTO in the subphase appeared very different from images of the plain DPPC film in Figure 3A, in good agreement with the different isotherm shape. The presence of G_{M1} /cholesterol forming “rafts” is quite evident. Even at very low film pressure, many small white domains likely representing “rafts” appear, surrounded by a gray background due to the DPPC “sea”. Dark zones indicating film holes are also present. The film compression leads to disappearance of these dark zones, to the formation of a lighter background, and to the formation of wide “rafts”.

Effects in the isotherms similar to those described for plain DPPC, although less accentuated, can be observed. Here, too, we observe a dose-dependent effect, but less than that observed on plain DPPC. The isotherms obtained after the TTO injection in the subphase have the collapse pressure of the lipid mixture without TTO, as observed for plain DPPC, suggesting that, even in this case, the films are made of DPPC/ G_{M1} /cholesterol. The main difference compared to the DPPC experiment is a reduced shift of the collapse onset. This effect is not evident at $X = 0.01$ and 0.02% , and only at $X = 0.04\%$ does the isotherm show a remarkable change of the collapse onset (from about 49 to 45 mNm). We can conclude that the occurrence of “rafts” in the model membrane stabilizes the lipid film. BAM images obtained in the presence of TTO in the subphase show many white features difficult to interpret even if whiter areas could be due to TTO molecules.

To better describe the interaction of TTO with model membranes, Figure 4 plots the film pressure change $\Delta\pi$ induced by the presence of TTO in the subphase versus the pressure film at which the TTO was injected π_i . A linear behavior can be observed for all the TTO concentrations and the kind of lipids used. Interestingly, the line for $X = 0.04$ is completely distinct from the other two in both kinds of lipids (black and orange).

The linear trend has been interpreted in the literature³⁵ as due to the dynamic absorption and penetration of the molecules of the subphase into the Langmuir film, and the extrapolation at $\Delta\pi = 0$ has been indicated as an important parameter π_0 describing the film stability. This parameter measures the monolayer compression needed to avoid the penetration of the TTO molecules into the Langmuir film: the more compact the film, the higher this value.

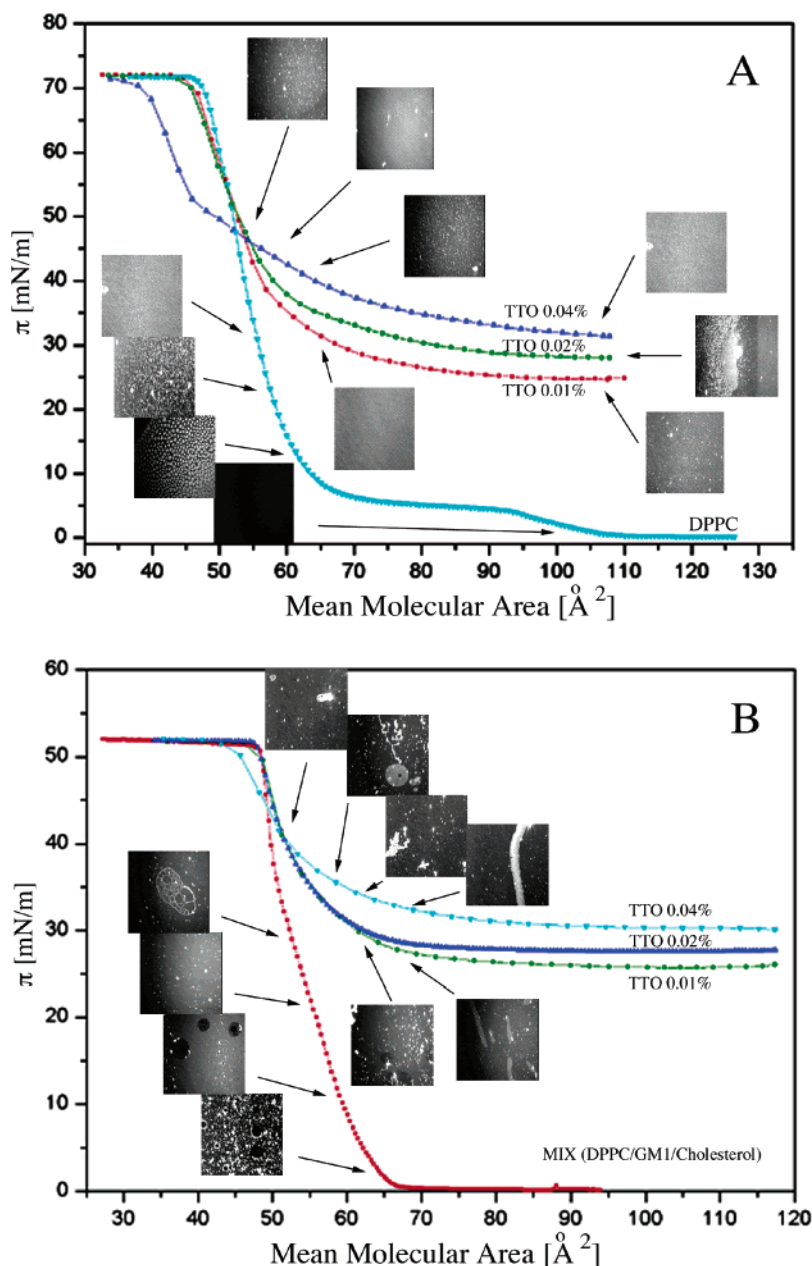


Figure 3. Compression isotherms with and without TTO in the subphase. (A) is relative to Langmuir films made of plain DPPC and (B) to mixed DPPC/G_{M1}/cholesterol simulating the “rafts” occurrence. The isotherms of the film without TTO and with three increasing TTO concentration are reported. BAM images show the monolayer morphology observed at the pressure indicated by the arrows.

In our opinion, the TTO interaction mechanisms with the two considered model membranes would be the same, but less effective, when lipid “rafts” are present. The inset of Figure 4, where π_0 is plotted versus the TTO concentration both for plain DPPC and DPPC/G_{M1}/cholesterol, supports this statement. It is worth observing that a linear behavior exists in the case of plain DPPC, indicating that the film needs to be more and more compressed to be insensitive to the presence of growing concentrations of TTO molecules in the water subphase. Conversely, this is not true in the case of DPPC/G_{M1}/cholesterol mixture, where π_0 is independent of the TTO concentration. This fact is due to the occurrence of the lipid “rafts” in the model membrane and demonstrates that the TTO molecules are less able to penetrate lipid “rafts” than the DPPC “sea”.

Freeze-Fracturing. Freeze-fracture technique allowed us to visualize both the protoplasmic face (PF) and exoplasmic face (EF) of the plasma membrane of P-gp positive M14 ADR cells

(Figure 5). Microvilli protruding from the cells were often observed (Figure 5A). As can be noted in Figure 5B, EF displayed a lower number of proteinaceous intramembrane particles (IMP) than PF (Figure 5A). However, the distribution of IMP appeared to be quite random in both faces.

“Rafts” were supposed to be mainly localized in the EF of the plasma membrane. In the EF of the control cells (Figure 5B), characteristic rounded domains, ranging in size from 10 to 100 nm, can be observed. Such domains, described by other authors as “caveolae”, may represent specialized membrane areas.⁴¹ “Caveolae” are formed from lipid “rafts” by polymerization of caveolins, integral membrane proteins that tightly bind cholesterol.²² This can be considered an indirect observation of “rafts”, even if not all “rafts” give rise to “caveolae” formation. Without labeling particular “rafts” components, such as cholesterol or gangliosides, the FF-TEM technique does not allow the direct visualization of “rafts”, because the membrane is

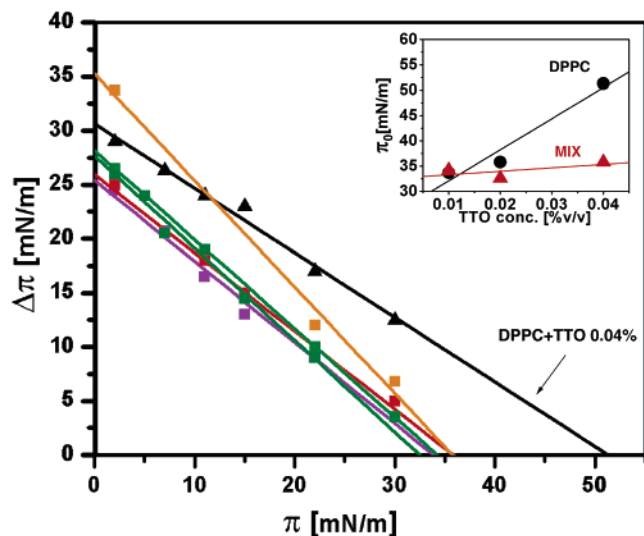


Figure 4. TTO adsorption kinetics. The variation of the monolayer pressure ($\Delta\pi$) induced by the presence of TTO in the subphase as a function of the initial compression pressure (π) is reported for plain DPPC (blue 0.01%; red 0.02%; black 0.04% v/v) and mixed DPPC/ G_{MI} /cholesterol film (green 0.01%, olive 0.02%; orange 0.04% v/v) simulating the “rafts” occurrence. The linear behavior is extrapolated to calculate π_0 , that is, the intersection with the x-axis, representing the compression pressure of the monolayer avoiding TTO penetration. The inset shows the comparison of the Langmuir film sensitivity to TTO representing the trends of the π_0 parameter versus the TTO concentration in the water subphase, in the case of plain DPPC (black) and mixed DPPC/ G_{MI} /cholesterol (red) film. As seen in the case of the occurrence of lipid “rafts”(MIX), the TTO concentration did not influence this parameter, indicating that the film is less sensitive to the oil action.

observed from the hydrophobic backbone. Unfortunately, “rafts” are mainly localized in the EF and protrude at the lipid–water interface.

Figure 6 shows the effects induced by the highest dose of TTO (0.04%) on the cell membrane. Even if TTO dramatically altered the morphology of the whole M14 ADR cells (data not shown), “caveolae” seem not to be influenced and are observed in both faces.

More interestingly, TTO induced the redistribution of the IMPs, with the formation of smooth IMP-free areas. The membrane proteins appeared to be clearly “clustered” in the PF (Figure 6A), indicating that the membrane molecular organization changed. Moreover, smooth plates of variable size and shape were detectable on both PF (Figure 6B, arrows) and EF (Figure 6C, arrows). The effect was more evident in the EF. The same areas, but narrower, were observed at lower oil concentrations (data not shown), demonstrating that this is a genuine effect induced by TTO. In our opinion these areas represent the direct visualization of the oil molecules which penetrated into the membrane and localized in the hydrophobic backbone. This is likely due to the affinity of the oil with the hydrophobic tails of lipids.

All these FF observations are in good agreement with all biophysical results. TTO interacts with the cell membrane penetrating through the less ordered lipid matrix, redistributes IMPs, does not alter the compact “rafts”/“caveolae” and, finally, accumulates in the hydrophobic zone of the membrane.

Flow Cytometry Analysis. To investigate the effect of TTO on the transport activity of P-gp, the uptake and efflux of an antitumoral drug (doxorubicin (DOX)) was analyzed by FCA in the absence and in the presence of TTO. In particular,

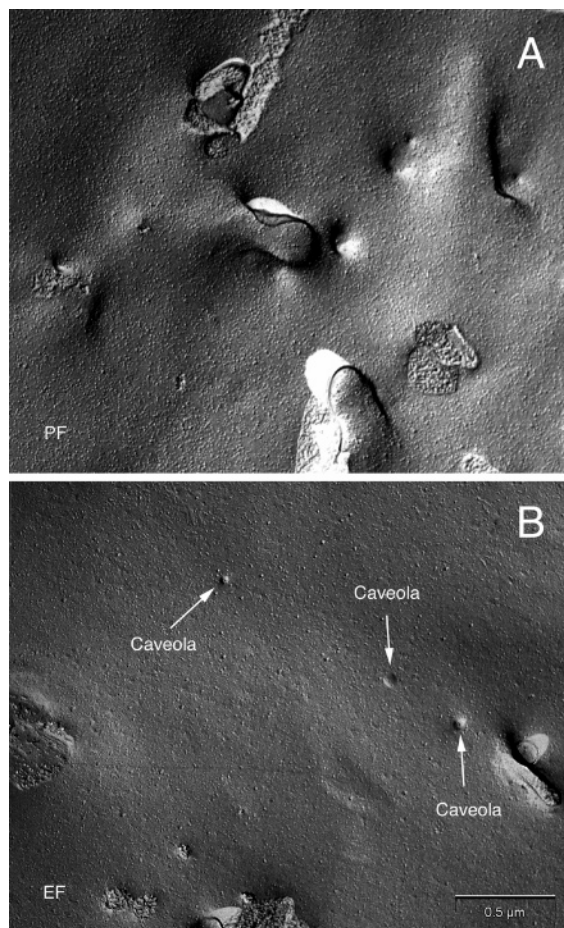


Figure 5. The plasma membrane structure of the control M14 MDR melanoma cells. Freeze-fracture transmission electron microscopy images of the control cell plasma membrane in the PF (A) and EF (B). IMPs are randomly distributed in both faces and “caveolae” can be easily observed in the EF (arrows).

experiments were performed on the drug-sensitive M14 WT cell line and its resistant counterpart M14 ADR.

M14 ADR cells express high levels of P-gp as proved by RT-PCR, Western blotting, and FCA.¹⁵ Moreover, as demonstrated by laser scanning confocal microscopy, most of the drug transporter is localized on the plasma membrane.

To verify if TTO modulates the functionality of P-gp, and taking into account the inherent fluorescence of DOX, accumulation and efflux studies of this antitumoral drug were performed by flow cytometry in the presence of TTO or cyclosporin-A (CsA), a known inhibitor of P-gp transport activity. M14 WT cells, which do not express the drug transporter on the plasma membrane, represented the internal negative control. For DOX accumulation studies, M14 cells were treated with 1.7 μ M DOX for 60 min in the presence or absence of CsA or TTO (0.005 and 0.01%). As shown in Figure 7A, the drug accumulated at lower extent in M14 ADR than sensitive cells. The presence of CsA significantly increased DOX uptake only in resistant cells, while TTO did not modify the pattern of drug accumulation.

For drug efflux studies, cells treated with DOX were allowed to recover in drug-free medium for 30 and 120 min in the presence or absence of CsA or TTO. In M14 WT cells, a certain amount of drug left the cells (probably due to passive efflux) after just 30 min of recovery, even in the presence of CsA and TTO (Figure 7B). In M14 ADR cells, fluorescence intensity due to accumulated drug decreased (from 11 to 4) during efflux

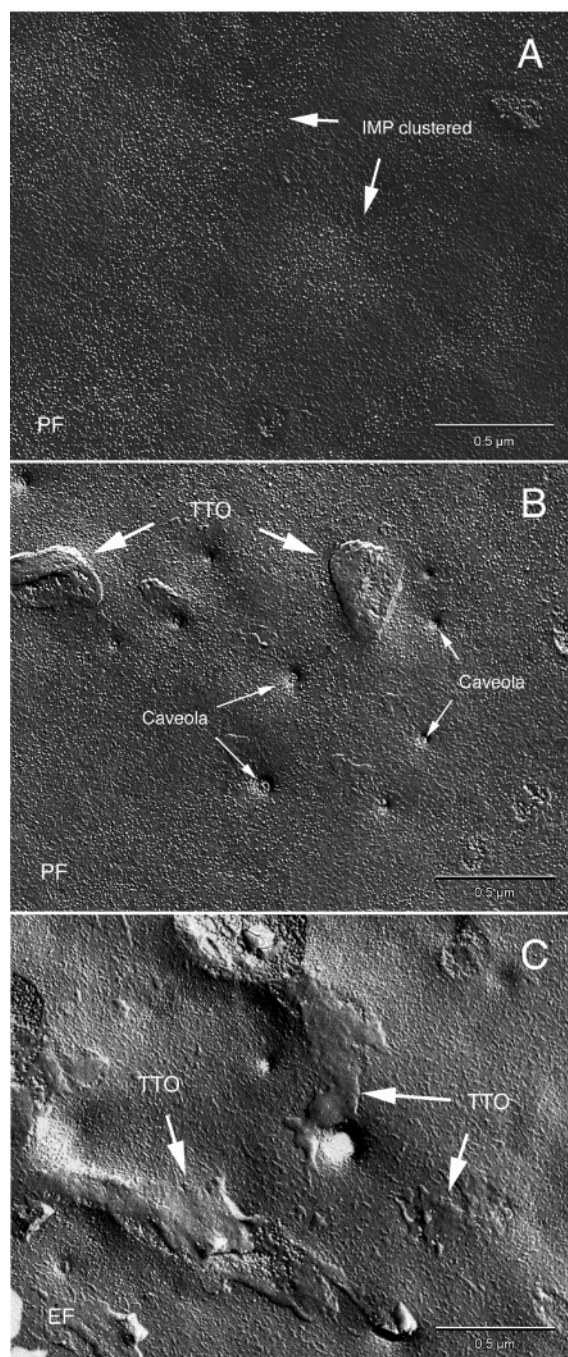


Figure 6. The plasma membrane structure of the TTO-treated M14 MDR melanoma cells. Freeze-fracture transmission electron microscopy images of cells treated with the maximum TTO concentration (0.04%). IMPs appear clustered and leave flat areas (A). TTO deposits can be observed in both faces (B, C) as smooth patches (arrows).

period. CsA clearly inhibited P-gp activity (as demonstrated by the increased fluorescence value when it was added to cells), while in the presence of TTO the P-gp extrusion activity was not altered. The same results were obtained after 120 min of efflux (data not shown).

All these results indicated that both the uptake and the efflux were not influenced by the presence of TTO; thus the ATPase-dependent transport function of P-gp seems not to be influenced by the interaction of the oil with the plasma membrane. Interestingly, our previous data¹⁵ demonstrated that in biological samples such as cultured human melanoma cells, TTO was able to impair cell growth, inducing caspase-dependent apoptosis. Remarkably, TTO proved to be more effective on

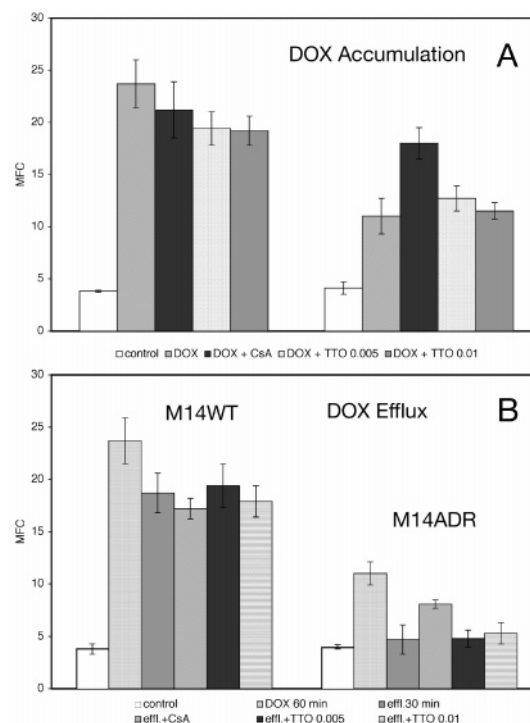


Figure 7. Flow cytometry analysis results. DOX accumulation (A) and efflux (B) in drug-sensitive and -resistant M14 melanoma cells.

MDR melanoma cells and to overcome P-gp mediated-resistance to apoptosis induced by certain stimuli. P-gp can inhibit nondrug apoptotic stimuli, including Fas and TNF, UVB- and gamma-irradiation, and serum starvation, by suppressing the activation of caspases.^{16,17} Recent data demonstrated that the antiapoptotic effect of P-gp is ATPase independent and a dual model for P-gp-induced MDR has been proposed involving both ATPase-dependent drug efflux and ATPase-independent inhibition of apoptosis.⁴²

Conclusions

Our biophysical experiments indicate that TTO interact with lipid "rafts" in a very different way than it does with plain DPPC "sea". In particular, TTO molecules were more easily able to interact with the DPPC monolayer than with the "rafts". This conclusion is in good agreement with the widely reported observation that lipid "rafts" are characterized by more compact lipid arrangements than the classic DPPC structure. These arrangements are due to the electrostatic interaction occurring between the charged headgroups of gangliosides and to the particular localization of the small cholesterol molecules inserted between the hydrophobic ganglioside tails. This structure is found to be in ordered phase even at temperature and compression values at which DPPC would be in LE phase.²²

Ultrastructural observations performed on freeze-fractured MDR cells confirmed the interaction of TTO with the plasma membrane. We observed a dose-dependent redistribution of IMP particles and a direct structural alteration of the cell membrane due to the oil. Finally, experiments performed by FCA demonstrated that the function of the MDR drug transporter P-gp was not interfered by TTO.

Accordingly to all data available in the literature and on the basis of our biophysical and biological results, we propose that the effect exerted on MDR cells by TTO might be mediated by its interaction with the fluid phase of the film, rather than with the more organized "rafts". This interaction should preferentially influence the ATP-independent antiapoptotic activity of P-gp,

likely localized outside “rafts” and “caveolae”. This hypothesis is in good agreement with the recent observation performed by Radeva et al.³² indicating the localization of P-gp outside the classic “rafts” containing G_{M1} and cholesterol.

Experimental Section

Materials. G_{M1}, DPPC and cholesterol were purchased from Sigma (Sigma Chemical Co., St. Louis, MO) with a purity of more than 99.9%. *Melaleuca alternifolia* essential oil (Pharmaceutical Grade) was kindly supplied by Dr. Giuseppe Salvatore of Department of “Ambiente e Connessa Prevenzione Primaria” of the “Istituto Superiore di Sanità”, Rome.

Langmuir Films: Sample Preparation and Thermodynamic Measurements. DPPC was dissolved in pure chloroform (1 mg·mL⁻¹). Mixed DPPC/G_{M1}/cholesterol solutions (1 mg·mL⁻¹) at a molar fraction of 49/4/47 mol % were dissolved in chloroform–methanol–water (1:2:0.15 v/v). Plain DPPC and mixed DPPC/G_{M1}/cholesterol monolayer were prepared at the air–water interface following the Langmuir technique.³⁵ Appropriate amounts of solution were spread with a microsyringe onto the aqueous subphase. To allow sufficient solvent evaporation, monolayers at the air–subphase interface rested about 10 min before compression. All experiments were carried out on a subphase constituted of distilled and deionized water produced by an ELIX3 (Millipore, Molsheim, France), thermostated by a water circulating bath (C25, Haake, Karlsruhe, Germany) at a temperature of 20.0 ± 0.2 °C.

The surface pressure–area isotherms were obtained by means of a computer-controlled commercial device model KSV3000 (Minitrough, KSV, Helsinki, Finland) enclosed in a Plexiglas box to reduce surface contamination. Symmetric compression was achieved with two moving barriers at a constant rate of 10 mm min⁻¹. The surface tension (π) of the lipid monolayer was measured using the Wilhelmy method, using a roughened platinum plate, with an accuracy of 1 mN m⁻¹.

Brewster Angle Microscopy. Brewster angle microscope visualized the morphology of the monolayer formed at the air–water interface. A model BAM2Plus NFT (NFT Gottingen, Germany) was mounted on a Langmuir trough model KSV3000 (KSV, Helsinki, Finland). The images were digitized using a frame grabber and treated with image-processing software to correct both distortions resulting from the observation at the Brewster angle and dishomogeneities in the laser illumination. The lateral resolution of the BAM can be estimated to be on the order of 3 μ m.

Cell Cultures. The established human melanoma cell line (M14 WT) and its derivative MDR variant (M14 ADR) were grown in RPMI 1640 medium (Flow Laboratories, Irvine, Scotland) supplemented with 1% nonessential amino acids, 1% L-glutamine, 100 IU/mL penicillin, 100 IU/mL streptomycin, and 10% fetal calf serum (Flow Laboratories, Irvine, Scotland) at 37 °C in a 5% CO₂ humidified atmosphere in air. M14 ADR cell line was cultured in the presence of 40 μ M doxorubicin (DOX) (Adriplastina, Pharmacia & Upjohn S.p.A., Milan, Italy).

Freeze-Fracture Transmission Electron Microscopy. For analyses on freeze-fractured replicas, cells were treated with 0.01, 0.02 or 0.04% TTO for 120 min, fixed with 2.5% glutaraldehyde in the culture medium immediately after the end of each treatment. After 20 min of fixation, cells were detached and centrifuged for 10 min at 1000 rpm, washed twice in Hank’s Balanced Salt Solution (HBSS), resuspended in the same medium containing 25% glycerol and incubated for 20 min at room temperature. The suspension was then centrifuged at 2000 rpm for 15 min, and the pellet was put on carriers and quickly frozen in Freon 22, partially solidified at the liquid nitrogen temperature. The mounted carriers were then transferred into a Bal-Tec BAF 060 freeze-etch unit (Bal-Tec Inc., Balzers, Liechtenstein), cleaved at -100 °C at a pressure of (2–4) × 10⁻⁷ mbar, shadowed with 2.5 nm of platinum–carbon, and replicated with 20 nm carbon film. Platinum–carbon evaporation (at an angle of 45°) and carbon evaporation (at an angle of 90°) were performed using electron beam guns; the thickness of the deposit was evaluated by means of a quartz crystal thin film

monitor. Cells were digested for 2 h from the replica by Clorox. The replicas were mounted on naked 300-mesh grids and examined with a Philips EM 208S Transmission Electron Microscope (FEI Company, Eindhoven, The Netherlands) at 60 kV.

Flow Cytometry Analysis. All flow cytometry analyses were carried out on cell suspensions (10⁶ cells/mL) obtained by incubating monolayer cell cultures with EDTA. The time course analysis of DOX uptake were performed on M14 WT and M14 ADR cells treated with 1.7 μ M DOX in culture medium for 60 min in the presence or absence of 5 μ M CsA (Sigma Chemical Co.) a known P-gp functionality modulator, or 0.01 and 0.005% TTO. At the end of the treatment, cells were washed with ice-cold HBSS (Sigma Chemical Co.), detached with EDTA, resuspended in ice-cold PBS, and immediately analyzed for the drug content. For drug efflux studies, cells were treated with DOX for 60 min, washed with ice-cold HBSS, and then reincubated at 37 °C in drug-free medium with or without CsA or TTO. Cells were washed and harvested for analysis after 30 and 120 min. Fluorescence signals were analyzed with a FACScan flow cytometer (Becton Dickinson, Mountain View, CA) equipped with a 15-mW, 488 nm, and air-cooled argon ion laser. DOX fluorescence emission was collected through a 575 nm band-pass filter and acquired in log mode. Drug fluorescence intensity was expressed as the Mean Fluorescence Channel (MFC).

Acknowledgment. This research was partially supported by a grant from the “Ministero della Salute” (1% Fondo Sanitario Nazionale).

References

- Brophy, J. J.; Davies, N. W.; Southwell, I. A.; Stiff, I. A.; Williams, L. R. Gas chromatographic quality control for oil of *Melaleuca terpinen-4-ol* type (Australian tea tree). *J. Agric. Food Chem.* **1989**, *37*, 1330–1335.
- Markham, J. L. Biological Activity of Tea Tree Oil. In *Tea Tree, the Genus Melaleuca*; Southwell I.; Lowe R., Eds.; Harwood Academic Publishers: Amsterdam, 1999; pp 169–190.
- Carson, C. F.; Riley, T. V. Antimicrobial activity of the major components of the essential oil of *Melaleuca alternifolia*. *J. Appl. Bacteriol.* **1995**, *78*, 264–269.
- Southwell, I. A.; Hayes, A. J.; Markham, J. L.; Leach, D. N. The search for optimally bioactive Australian tea tree oil. *Acta Hort.* **1993**, *334*, 265–275.
- Altman, P. M. Australian tea tree oil. *Aust. J. Pharm.* **1988**, *69*, 276–278.
- Anderson, J. N.; Fennessy, P. A. Can tea tree (*Melaleuca alternifolia*) oil prevent MRSA? *Med. J. Aust.* **2000**, *173*, 489–456.
- Caelli, M.; Porteous, J.; Carson, C. F.; Heller, R.; Riley, T. V. Tea tree oil as an alternative topical decolonization agent for methicillin-resistant *Staphylococcus aureus*. *J. Hosp. Infect.* **2000**, *46*, 236–237.
- Carson, C. F.; Riley, T. V.; Cookson, B. D. Efficacy and safety of tea tree oil as a topical antimicrobial agent. *J. Hosp. Infect.* **1998**, *40*, 175–178.
- May, J.; Chan, C. H.; King, A.; Williams, L.; French, G. L. Time-kill studies of tea tree oils on clinical isolates. *J. Antimicrob. Chemother.* **2000**, *45*, 639–643.
- Zhang, S. Y.; Robertson, D. A study of tea tree oil ototoxicity. *Audiol. Neurootol.* **2000**, *5*, 64–68.
- D’Auria, F. D.; Laino, L.; Strippoli, V.; Tecca, M.; Salvatore, G.; Battinelli, L.; Mazzanti, G. In vitro activity of tea tree oil against *Candida albicans* mycelial conversion and other pathogenic fungi. *J. Chemother.* **2001**, *13*, 377–83.
- Ernst, E.; Huntley, A. Tea tree oil: a systematic review of randomized clinical trials. *Forsch. Komplementarmed. Klass. Naturheilkd.* **2000**, *7*, 17–20.
- Nenoff, P.; Hausteil, U.; Brandt, W. Antifungal activity of the essential oil of *Melaleuca alternifolia* (tea tree oil) against pathogenic fungi in vitro. *Skin Pharmacol.* **1996**, *9*, 388–394.
- Syed, T. A.; Qureshi, Z. A.; Ali, S. M.; Ahmad, S.; Ahmad, S. A. Treatment of toenail onychomycosis with 2% butenafine and 5% *Melaleuca alternifolia* (tea tree) oil in cream. *Trop. Med. Int. Health* **1999**, *4*, 284–287.
- Calcabrini, A.; Stringaro, A.; Toccaceli, L.; Meschini, S.; Marra, M.; Colone, M.; Salvatore, G.; Mondello, F.; Arancia, G.; Molinari, A. Terpinen-4-ol, the main component of *Melaleuca alternifolia* (tea tree) oil inhibits the in vitro growth of human melanoma cells. *J. Invest. Dermatol.* **2004**, *122*, 349–60.

- (16) Smyth, M. J.; Krasovskis, E.; Sutton, V. R.; Johnstone, R. W. The drug efflux protein, P-glycoprotein, additionally protects drug-resistant tumor cells from multiple forms of caspase-dependent apoptosis. *Proc. Natl. Acad. Sci. U.S.A.* **1998**, *95*, 7024–7029.
- (17) Johnstone, R. W.; Cretne, y E.; Smyth, M. J. P-glycoprotein protects leukemia cells against caspase-dependent, but not caspase-independent, cell death. *Blood* **1999**, *93*, 1075–1085.
- (18) Gollapud, S.; Gupta, S. Anti-P-glycoprotein antibody-induced apoptosis of activated peripheral blood lymphocytes: a possible role of P-glycoprotein in lymphocyte survival. *J. Clin. Immunol.* **2001**, *21*, 420–430.
- (19) Singer, S. J.; Nicolson, G. L. The fluid mosaic model of the structure of cell membranes. *Science* **1972**, *175*, 730–731.
- (20) Thompson, T. E.; Tillack T. W. Organization of glycosphingolipids in bilayers and plasma membranes of mammalian cells. *Annu. Rev. Biophys. Biophys. Chem.* **1985**, *14*, 361–86.
- (21) Simons K.; Ikonen E. Functional rafts in cell membranes. *Nature* **1997**, *387*, 569–572.
- (22) Simons K.; Toomre D. Lipid rafts and signal transduction. *Nature Rev.* **2000**, *1*, 31–39.
- (23) Simons K.; Ikonen E. How cells handle cholesterol. *Science* **2000**, *290*, 1721–1726.
- (24) Rinia H. A.; de Kruijff B. Imaging domains in model membranes with atomic force microscopy. *FEBS Lett.* **2001**, *25113*, 1–6.
- (25) Yuan C.; Johnston L. J. Distribution of ganglioside G_{M1} in L- α -DPPC/Cholesterol monolayers: a model for lipid rafts. *Biophys. J.* **2000**, *79*, 2768–2781.
- (26) Yuan C.; Johnston L. J. Atomic force microscopy studies of ganglioside G_{M1} in phosphatidylcholine and phosphatidylcholine/Cholesterol bilayers. *Biophys. J.* **2001**, *81*, 1059–1069.
- (27) Yuan C.; Furlong J.; Burgos P.; Johnston L. J. The size o lipid rafts: an atomic force microscopy study of ganglioside G_{M1} domains in sphingomyelin/DOPC/cholesterol membranes. *Biophys. J.* **2002**, *82*, 2526–2535.
- (28) Tsui-Pierchala B. A.; Encinas M.; Milbrandt J.; Johnson E. M. J. Lipid rafts in neuronal signaling and function. *Trends Neurosci.* **2002**, *25*, 412–417.
- (29) Lavie Y.; Fiucci G.; Czarny M.; Liscovitch M. Changes in membrane microdomains and caveolae constituents in multidrug-resistant cancer cells. *Lipids* **1999**, *34*, Suppl. S57–63.
- (30) Bacso Z.; Nagy H.; Goda K.; Bene L.; Fenyvesi F.; Matko J.; Szabo G. Raft and cytoskeleton associations of an ABC transporter: P-glycoprotein. *Cytometry* **2004**, *61A*, 105–116.
- (31) Troost J.; Lindenmaier H.; Haefeli W. E.; Weiss J. Modulation of cellular cholesterol alters P-glycoprotein activity in multidrug-resistant cells. *Mol. Pharmacol.* **2004**, *66*, 1332–1336.
- (32) Radeva G.; Perabo J.; Sharom F. J. P-Glycoprotein is localized in intermediate-density membrane microdomains distinct from classical lipid rafts and caveolar domains. *FEBS J.* **2005**, *272*, 4924–4937.
- (33) Diociaiuti M.; Bordi F.; Motta A.; Carosi A.; Molinari A.; Arancia G.; Coluzza C. Aggregation of gramicidin A in phospholipid Langmuir–Blodgett monolayers. *Biophys. J.* **2002**, *82*, 3198–3206.
- (34) Diociaiuti M.; Ruspantini I.; Giordani C.; Bordi F.; Chistolini P. Distribution of GD3 in DPPC monolayers: a thermodynamic and atomic force microscopy combined study. *Biophys. J.* **2004**, *86*, 321–328.
- (35) Roberts G. *Langmuir–Blodgett films*; Plenum Press: New York, 1990.
- (36) Honig D.; Mobius J. Direct visualization of monolayers at the air–water interface by Brewster angle microscopy. *J. Phys. Chem.* **1991**, *95*, 4590–4592.
- (37) Leporatti S.; Brezesinski G.; Mohwald H. Coexistence of phases in monolayers of branched-chain phospholipids investigated by scanning force microscopy. *Colloids Surfaces A* **2000**, *161*, 159–171.
- (38) Kaganer V. M.; Mohawald H.; Dutta P. Structure and phase transitions in Langmuir monolayers. *Rev. Mod. Phys.* **1999**, *71*, 779–818.
- (39) Luckham P.; Wood J.; Froggatt S.; Swart R. The surface properties of gangliosides. *J. Colloid Interface Sci.* **1993**, *156*, 164–172.
- (40) Dynarowicz-Latka P.; Dhanabalan A.; Oliveira Jr. O. N. Modern physicochemical research on Langmuir monolayers. *Adv. Colloid. Interface Sci.* **2001**, *91*, 221–293.
- (41) Robenek M. J.; Schlattmann K.; Zimmer K. P.; Plenz G.; Troyer D.; Robenek H. Cholesterol transporter caveolin-1 transits the lipid bilayer during intracellular cycling. *FASEB J.* **2003**, *17*, 1940–1942.
- (42) Tainton K. M.; Smyth M. J.; Jackson J. T.; Cerruti L.; Jane S. M.; Darcy P. K.; Johnstone R. W. Mutational analysis of P-glycoprotein: suppression of caspase activation in the absence of ATP-dependent drug efflux. *Cell Death Differ.* **2004**, *11*, 1028–1037.

JM060228I